STEERING STABILITY ANALYSIS AND CONTROL STRATEGY OF THE SIX WHEEL-LEGGED CHASSIS FOR FOREST

Cheng YUJING[1] Wang DIAN*[2] Liu JINHAO[3] Huang QINGQING[4]

In order to increase the steer stability of the six wheel-legged chassis on forest slope. [Method] The stability model of the six-wheel legged chassis using the spin theory is established in this paper. On the slope with a maximum inclination of 30°, the stabilities of the six-wheel legged chassis with a maximum steering angle of 30° and a maximum speed of 9m/s are simulated and calculated. Aiming at the critical rollover state, a control model of the swing arm hydraulic cylinders of six-wheel legged chassis is proposed, and the response function of the swing arm hydraulic cylinders in the critical rollover state is calculated. [Result and conclusion] The calculation and experiment result show that when the speed is higher than 8m/s and the steering angle is bigger than 25°, the chassis reaches the critical rollover state. By adjusting the work of swing arm hydraulic cylinders, the stability is increased from -0.2 to 0.3 when the steering angle is 30° and the speed is 9m/s.

Key words: forest six-wheel legged chassis; rollover stability; turning; controlling strategy

1.Introduction

In recent years, in order to rapidly improve the mechanization level of forest areas in China and improve the operating conditions of forest areas machinery, it is extremely necessary for forest areas to develop a chassis suitable for forest areas[1-3]. The six-wheel legged chassis for forests can actively overcome obstacles and level steering in rough forest terrain. Finding the stability theory applicable to the forest chassis and developing a useful control strategy have great significance to improve the stability of the six-wheel legged chassis when performing steering operations on forest slopes[4-5]. After measurement of steady-state edge angle by Zhu Qingyuan, steady-state edge angle could be the standard of rollover stability[6]. Using the potential field function to judge the rollover stability index based on the information of lateral acceleration and measured roll angle by Mian Ashfaq Ali et

[1] Eng., Dept. of Technology, Beijing Forestry University, e-mail: ching_yj@163

[2] Reader, Dept. of Technology, Beijing Forestry University, e-mail: wangdian@bjfu.edu.cn

[3] Prof., Dept. of Technology, Beijing Forestry University, e-mail: liujinhao@bijfu.edu.cn

[4] Reader, Dept. of Technology, Beijing Forestry University, e-mail: huangqingqing@bijfu.edu.cn

al[7]. Li Xuefei and Yao Zongwei determined the rollover stability of wheel loaders through the two-level stability theory and controlled the leveling by fuzzy neural theory[8-10]. Longitudinal stability and the vertical slip angle are used to judge the stability of the tractor chassis by Ouyang Yibin et al[11]. Tian Haibo and others combined the dynamic energy stabilization boundary method with the stable cone method to obtain the dynamic energy stabilization cone method, furthermore, evaluating the rollover stability of a robot with six configurations by this method[12-13]. For the mountain tractor, Wang Zhongshan of Jilin University designed a leveling hydraulic system for self-adjusting of the body attitude[14]. Through the curves of the flow, pressure, displacement and speed of the piston rod of the hydraulic cylinder in the hydraulic system, learned that the stability of the body leveling hydraulic system can meet the working requirements under the mountain slope inclination ≤15 °working conditions. Cao Shikai of Northeast Forestry University designed a car scanner on-board leveling mechanism. Through the laser scanner's collection and analysis of slope angle, bush height, tree height, and tree coordinates, the angle of the leveling platform was determined[15].

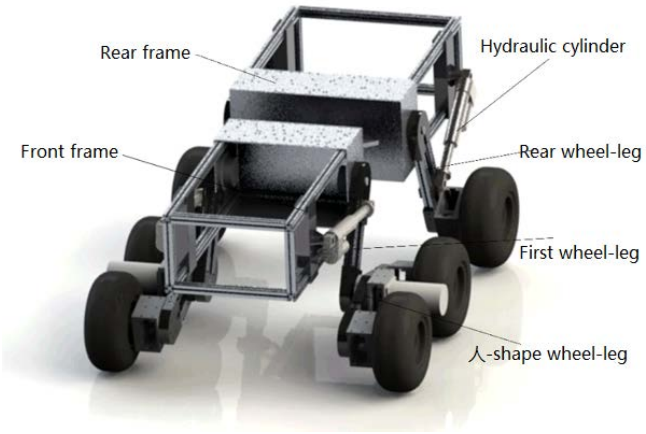

Fig.1 Virtual prototype of wheel-leg chassis in Solid works

Table1

Parameter for the prototype chassis

Parameter	Data	Unit
Track (2a)	1.026	m
The distance from the articulated shaft to the articulated point of the front frame (b)	0.328	m
rear wheel-leg (l_1)	0.439	m

front upper wheel-leg (l_2)	0.467	m
人-shape wheel-leg (l_3)	0.311	m
人-shape wheel-leg angle (φ)	153	degree
Rear wheel-legs swing angle range (θ_1, θ_2)	33.3~67	degree
front upper wheel-legs swing angle range (θ_3, θ_4)	26~51	degree
人-shape wheel-legs swing angle range (θ_5, θ_6)	37.8~51.8	degree
Articulated steering angle (γ)	-30~30	degree

Consequently, the chassis quality was optimized, and a virtual prototype of the forest six-wheel legged chassis was established. The prototype model are shown in Figure 1, where the hydraulic cylinder diameter is D = 80mm, thrust is 70KN, rod diameter is d = 55mm, and pull is 37KN.

In addition, in this paper, a chassis stability model is established for a forest six-wheel legged chassis. The control model of the legged hydraulic cylinder is established to realize anti-rollover of the chassis and improve its steering stability.

2. Six-wheel legged chassis stability model

Aiming at the virtual prototype, the kinematics equations of the six-wheel legged chassis during the movement of the chassis are established based on the screw theory[16-20]. Using the positive solution exponential product formula of robot kinematics, the kinematics equation of the six-wheel legged chassis moving from the initial base coordinate system to the end tool coordinate system can be obtained:

$$g_{03}(\theta_1,\theta_2,...,\theta_n) = e^{\hat{\xi}_1\theta_1}\cdot e^{\hat{\xi}_2\theta_2}\cdot ...\cdot e^{\hat{\xi}_n\theta_n} \tag{1}$$

Among them, $g = e^{\hat{\xi}\theta}$ is the motion transformation matrix of each rigid body, and θ is the swing angle range of the wheel-leg, $\xi = \begin{bmatrix} \dot{\nu} & \omega \end{bmatrix} \in R^{6\times1}$ is the motion screw coordinate, and $g_{03}(\theta_1,\theta_2,...,\theta_n)$ is the motion change matrix of the whole

part in the base coordinate system.

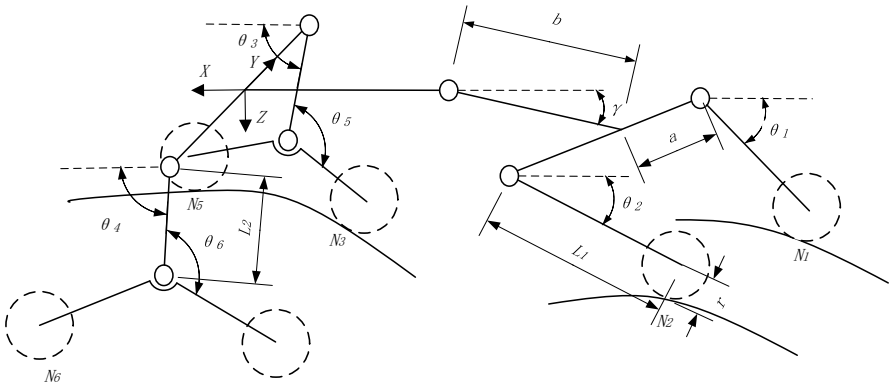

Fig.2 Structure and parameters of 6 wheel-legged chassis

The kinematics matrix of rotation and translation of each wheel-leg around the base coordinate is solved by formula(1). Thinking of the right first wheel-leg and the 人-shape wheel-leg of the front frame as a whole, followed by the left first wheel-leg and the 人-shape wheel-leg of the front frame, the articulated steering angle γ and the right wheel-leg of the rear frame, the articulated steering angle γ and the left wheel-leg of the rear frame. The positive solution exponential product formula are used to obtain the position and posture changes of each integral part during rotation and translation. Therefore, the kinematic change matrix of the base coordinate system to the end of the tire ground point could be obtained, and finally the coordinates of the chassis tire ground point can be calculated, which can be expressed in $T = e^{\hat{\xi}\Delta\theta} e^{\hat{\xi}\Delta\theta}$ direction as follows

$$T_3 = e^{\hat{\xi}_1 \Delta\theta_3} e^{\hat{\xi}_2 \Delta\theta_5} = \begin{bmatrix} \cos(\Delta\theta_3 - \Delta\theta_5) & 0 & -\sin(\Delta\theta_3 - \Delta\theta_5) & -l_2(\cos(\Delta\theta_3 - \Delta\theta_5) - \cos\Delta\theta_3 \\ 0 & 1 & 0 & 0 \\ \sin(\Delta\theta_3 - \Delta\theta_5) & 0 & \cos(\Delta\theta_3 - \Delta\theta_5) & -l_2(\sin(\Delta\theta_3 - \Delta\theta_5) - \sin\Delta\theta_3 \\ 0 & 0 & 0 & 1 \end{bmatrix}$$

$$T_5 = e^{\hat{\xi}_1 \Delta\theta_4} e^{\hat{\xi}_2 \Delta\theta_6} = \begin{bmatrix} \cos(\Delta\theta_4 - \Delta\theta_6) & 0 & -\sin(\Delta\theta_4 - \Delta\theta_6) & -l_2(\cos(\Delta\theta_4 - \Delta\theta_6) - \cos\Delta\theta_4 \\ 0 & 1 & 0 & 0 \\ \sin(\Delta\theta_4 - \Delta\theta_6) & 0 & \cos(\Delta\theta_4 - \Delta\theta_6) & -l_2(\sin(\Delta\theta_4 - \Delta\theta_6) - \sin\Delta\theta_4 \\ 0 & 0 & 0 & 1 \end{bmatrix} \quad (2)$$

(3)

$$T_1 = e^{\hat{\xi}_3 \Delta\gamma} e^{\hat{\xi}_4 \Delta\theta_1} = \begin{bmatrix} \cos\Delta\gamma\cos\Delta\theta_1 & -\sin\Delta\gamma & \cos\Delta\gamma\sin\Delta\theta_1 & b(\cos\Delta\gamma-1)+2b\cos\Delta\gamma(\cos\Delta\theta_1-1) \\ \sin\Delta\gamma\cos\Delta\theta_1 & \cos\Delta\gamma & \sin\Delta\gamma\sin\Delta\theta_1 & b\sin\Delta\gamma(2\cos\Delta\theta_1-1) \\ -\sin\Delta\theta_1 & 0 & \cos\Delta\theta_1 & -2b\sin\Delta\theta_1 \\ 0 & 0 & 0 & 1 \end{bmatrix}$$

(4)

$$T_2 = e^{\hat{\xi}_3 \Delta\gamma} e^{\hat{\xi}_4 \Delta\theta_2} = \begin{bmatrix} \cos\Delta\gamma\cos\Delta\theta_2 & -\sin\Delta\gamma & \cos\Delta\gamma\sin\Delta\theta_2 & b(\cos\Delta\gamma-1)+2b\cos\Delta\gamma(\cos\Delta\theta_2-1) \\ \sin\Delta\gamma\cos\Delta\theta_2 & \cos\Delta\gamma & \sin\Delta\gamma\sin\Delta\theta_2 & b\sin\Delta\gamma(2\cos\Delta\theta_2-1) \\ -\sin\Delta\theta_2 & 0 & \cos\Delta\theta_2 & -2b\sin\Delta\theta_2 \\ 0 & 0 & 0 & 1 \end{bmatrix}$$

(5)

When the forest six-wheel legged chassis is steered on an inclined plane. The articulated steering angle and the tilt axis connected in the middle of the front and rear frames on the same side are not conducive to the stability of the chassis, while the contralateral side is conducive to the stability of the chassis, this means that this article only considers the rollover condition of the chassis turning below the slope.

As the average slope of the forest area is 26.6 °[25], steep slopes of 30 ° ~ 45 ° are formed in small sections[26]. For adapting to the forest, a six-wheel legged chassis is used to drive on the slope of the southeast forest area, the stability calculation is performed by using the second-level stability theory and the steering stability of the chassis on the limit 30 ° slope is simulated[21-23], α=30° .

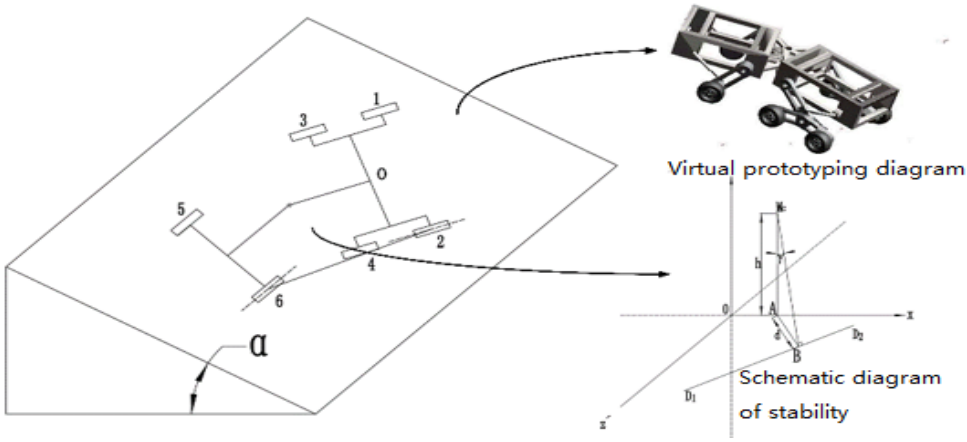

Fig.3 Six wheel-leg chassis down steering condition on the slope

When the tilt axis and the articulated steering angle of the chassis are on the same side, it against stability of the chassis, and when it is on the opposite side, it can better balance the stability of the chassis[16-17]. As shown in Fig. 3, 1-6

represents the coordinates of the 6 tire contact points of the chassis. M_C is the barycentric-coordinate of the chassis, 'h' is the distance from the barycentric to the ground, D_1, D_2 are the tilt axis when the chassis is tipped, that is, the line where the ground contact position of the 2,6 tire is located, and 'd' is the projection of the M_C barycentric onto the ground to the tilt axis. γ is the angle of stability.

With the continuous movement of the chassis on the slope, the γ angle changes with the change of the center of gravity. The stability $\tan\gamma = i = d/h$ can subsequently be expressed as: $i > 0$, the chassis is in a stable state; $i = 0$, the chassis is in a critical state; $i < 0$, the chassis is in a roll-over conditions. The stability function can be expressed as

$$i = \frac{\left|\begin{array}{l}(0.0355\cos\theta_1 + 0.0178 - 0.0458\cos\theta_2 + 0.0035\cos\theta_3 + 0.0481\cos\theta_5 - 0.0807\cos\theta_6 + 0.018\sin\theta_1 \\ +0.0799\sin\theta_5 + 0.0801\sin\theta_6)(0.283\sin\theta_4 - 0.189\sin\gamma - 0.074\sin\gamma\cos\theta_2 + 0.111\cos\theta_2\sin\theta_4 \\ -0.111\cos\theta_2\sin\theta_2 + 0.105\cos\theta_2 - 0.225\sin\theta_2) - (0.0799\cos\theta_5 + 0.0801\cos\theta_6 - 0.0619\sin\theta_1 \\ -0.0619(\sin\theta_1 + \sin\theta_2) - 0.0485\sin\theta_5 + 0.0807\sin\theta_6)(0.284\cos\theta_4 + 0.189\cos\gamma + 0.197 \\ +0.112\cos\theta_4\cos\theta_2 + 0.074\cos\gamma + 0.267\cos\theta_2)\end{array}\right|}{\sqrt{\left|0.46\cos\theta_4 + 0.311\cos\gamma + 0.32 + 0.36\cos^2\theta_2\right|^2 + \left|0.095 + 0.23\cos^2\theta_6\right|^2 + \left|-0.467\sin\theta_4 + 0.311\sin\gamma - 0.328 + 0.439\sin\theta_2\right|^2}} - \alpha \tag{6}$$

3. Six-wheel legged chassis full load rollover stability

When the six-wheel legged chassis is traveling along a horizontal slope, two factors, the forward speed and the folded-back steering angle, may cause the stability of the chassis to fluctuate [9,10]. Consequently, when steering under full-load conditions of the chassis, the influence of the articulated steering angle and the forward speed on the stability of the chassis are discussed.

According to formula $\frac{m_c \cdot v_x^2}{r} \cdot l_q \geq m_c g \cdot l_w$, it can be inferred that the maximum chassis speed is 8.3m/s when the stabilizing moment is equal to the tilting moments, so the maximum chassis speed used in the simulation is 9m/s. According to terrain mechanics and finite element analysis, the force that each wheel-leg can withstand is calculated, the body weight and load weight are evenly distributed to each wheel-leg. Finally, the virtual prototype load of the six-wheel legged chassis

in the forest area is fully loaded to 960Kg. Under normal driving conditions, the articulated steering angle of the front and rear frames is 30 °that do not affect each other. Under the conditions of the maximum articulated turning angle of 30 degrees, the forward speeds are 5m/s, 6m/s, 7m/s, 8m/s, 9m/s. Through simulation, the steering angle and stability curve at different forward speeds can be output under full load conditions.

It can be seen from Figure 4 that when the six-wheel legged chassis steering on the slope at a 30 ° articulated steering angle, the output stability indicates that the chassis is still stable when the speed is 7m/s, the threshold is reached at a speed of 8m/s, and the chassis rolls over at 9m/s. Therefore, when the turning angle is 25 °, it only needs to simulate the working conditions of the forward speed of 8m/s and 9m/s for comparison.

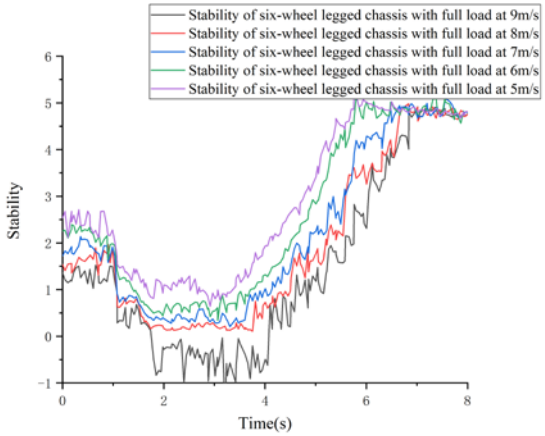

Fig.4 Stability at different speeds when the waist is turned to 30°

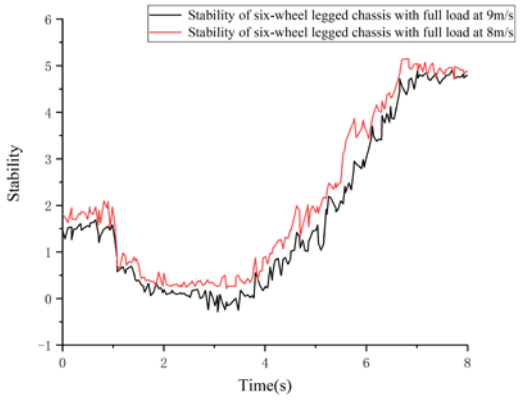

Fig.5 Stability at different speeds when the waist is turned to 25°

From Figure 5, it can be seen that while the six-wheel legged chassis is traveling horizontally on the slope and turning to the left in the forward direction, when the articulated steering angle reaches 25 ° and the forward speed reaches 8m/s, the chassis is in a stable state; when the forward speed reaches 9m/s, the chassis will roll over, and the minimum stability at this time is -0.2.

4. Rollover stability of six-wheel legged chassis under control conditions

The position of the wheel-leg affects the performance when the six-wheel legged chassis run in uneven road. A simplified model that presents working condition is shown in Figure 6, Figure 6 presents the wheel-leg and the frame with lifting and dropping which is completed by the extension and contraction of the hydraulic cylinder[24]. (the wheel-legs work principle is similar). The extension and contraction of the hydraulic cylinder during the working cause the angle θ between the wheel-leg and the frame in the base coordinate system to change, so stability $_i$ changes. The range of point A that presents the position of wheel-leg can be acquires. Especially, point D is the origin of coordinates. By establishing the geometric relationship, it is possible to obtain the relationship between the change of the wheel-leg angle caused by the lifting and dropping of the wheel legs and the change of the frame position.

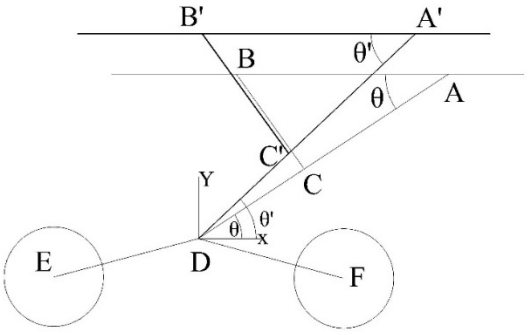

Fig.6 The lifting and dropping position changed of hydraulic cylinder

Through the analysis of geometric figure relations, the relationship between the wheel-leg swing angle change $\Delta\theta$ and the change in the hydraulic cylinder can be expressed as

$$\theta = \arccos\frac{AB^2 + AC^2 - BC^2}{2 \times AB \times AC} \tag{7}$$

$$\theta' = \arccos\frac{AB^2 + AC^2 - B'C'^2}{2 \times AB \times AC} \tag{8}$$

$$\Delta\theta = \theta - \theta' \tag{9}$$

$$B'C'^2 = AB^2 + AC^2 - 2 \times AB \times AC \times COS\theta' \tag{10}$$

$$BC^2 = AB^2 + AC^2 - 2 \times AB \times AC \times COS\theta \tag{11}$$

Consequently, the relationship between the change amount in the rotation angle of the wheel-leg $\Delta\theta$ and the change amount in the frame lifting or dropping Δy can be calculated as

$$\Delta y = AD \times \sin(\arccos\frac{AB^2 + AC^2 - BC^2}{2 \times AB \times AC}) - A'D \times \sin(\arccos\frac{AB^2 + AC^2 - BC^2}{2 \times AB \times AC} - \Delta\theta) \tag{12}$$

When $\Delta\theta$ is positive, the hydraulic cylinder is extended, the frame is raised, and the swing angle is increased. When $\Delta\theta$ is negative , the hydraulic cylinder is contracted, the frame is lowered, and the rotation angle is reduced. Equation (12) can inversely solve the change amount of the wheel-leg angle by the height of the frame lifting and dropping, and then the amount of extension and contraction of the hydraulic cylinder can be calculated.

The fuzzy control combined with the inverse solution function of the six-wheel legged chassis wheel-leg hydraulic cylinder controls the cylinder length and telescopic speed to obtain the required motion effect. Based on the combination of Simulink and Adams, the model in Adams is imported into the Matlab/Simulink environment, as shown in Figure 7, the inputs of the Adams include the forward speed and the articulated steering angles. The outputs of the Adams are stability, cylinder length. The table of fuzzy control rules of rear wheel-leg for four wheel-leg hydraulic cylinders is shown in Table 2.

Table2. Fuzzy control rule table

L / t	L1	L2	L3	L4	L5	L6	L7
SPEED	M	M	NS	NS	NS	NB	NB
FIRST	PS	M	NS	NB	NB	NB	NB
SECOND	PS	PS	PS	M	NS	NB	NB
END	PB	PS	PS	M	NS	NB	NB

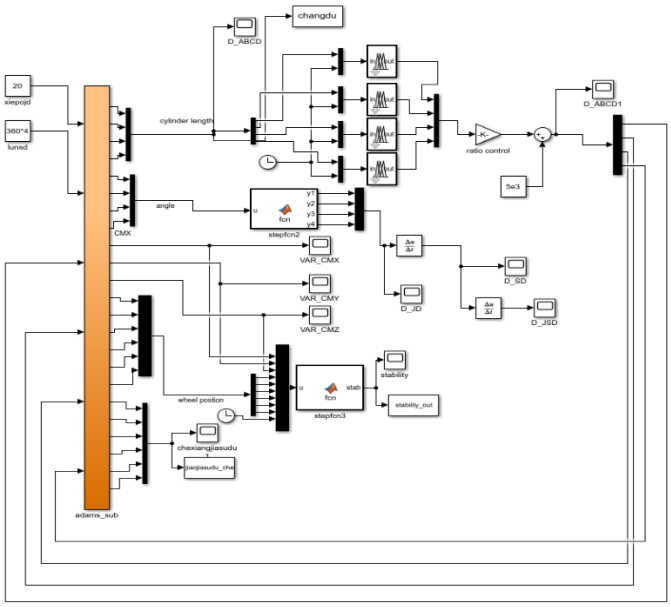

Fig.7 Adams and Simulink co-simulation

The chassis stability of the output under PID control and fuzzy control is compared with the stability without control, and the following sets of data are obtained, which means the stability changes under different steering angles.

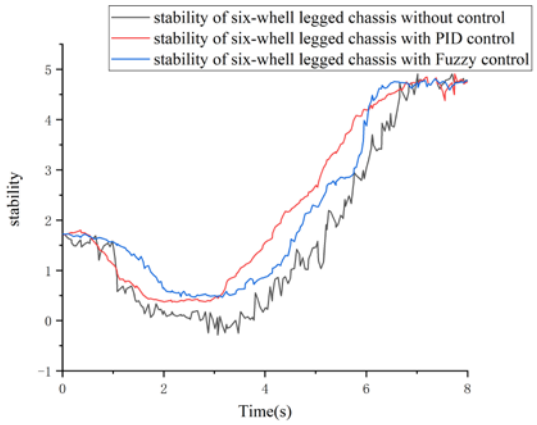

Fig.8 The front and rear frame stability changes in 25° steering angle with different forward speed.

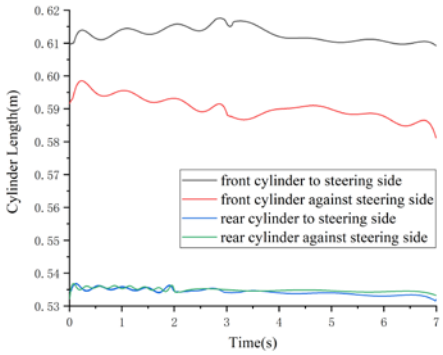

Fig.9 The variation curve of hydraulic cylinder length on the condition of 25° steering angle

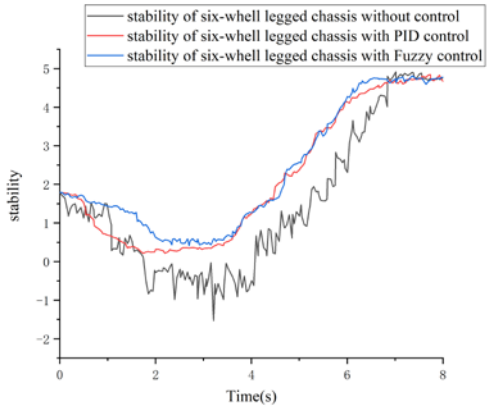

Fig.10 The front and rear frame stability changes in 30° steering angle with different forward speed.

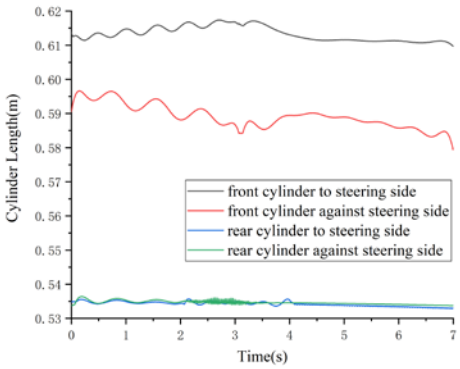

Fig.11 The variation curve of hydraulic cylinder length on the condition of 30° steering angle

As shown in Figures 8 and 10, when the six-wheel legged chassis forward speed is 9m / s, and the steering angles are 25° and 30°, respectively, comparing the three stability change curves, it is found that the stability under fuzzy control is better than that of PID control, the hydraulic cylinder response under fuzzy control is slower than PID control, and the frame fluctuation is also slow, these data indicate that the control strategy of the six-wheel legged chassis for the forest road with a slope of 30° works, furthermore, which is beneficial to improving the drive's comfort.

After the six-wheel legged chassis is added with fuzzy control, the stability under the 25° articulated steering angle is improved by approximately 3% compared with the PID control. According to Figure 9, the variation range of the inner hydraulic cylinder is 61.0cm to 61.6cm, and the variation range of the outer hydraulic range is 58.7cm to 59.8cm. Under the working condition of the 30 ° articulated steering angle, the stability has been improved by approximately 2%. It can be seen from Figure 11 that the variation range of the inner hydraulic cylinder is 61.2 cm to 61.8 cm, and the variation range of the outer hydraulic cylinder is 58.5 cm to 59.6 cm.

5.Conclusions

1)The kinematics model of the forest six-wheel legged chassis is established based on the screw theory. The stability of the forest six-wheel legged chassis is calculated by the kinematics model and the second-level stability theory, moreover, the simulation data is substituted into the theoretical equation to solve the stability under full load conditions.

2)Aiming at the working conditions with large fluctuations in stability and the possibility of overturning, a control model of the six-wheel legged chassis wheel-leg hydraulic cylinder was set up when the forest six-wheel legged chassis was steered on a 30 ° slope. Adams / Simulink co-simulation with fuzzy control was established.

3) When there is no control strategy, the maximum driving speed of the six-wheel legged chassis under full load is 8m/s. After adding the control strategy, under the condition that the vehicle speed is 9m/s and the articulated steering angle is 25 °, the minimum chassis stability is approximately 0.371, which is about 13% improvement. When the articulated steering angle is 30 °, the minimum stability of the chassis is approximately 0.214, and the overall stability has been improved by 10%. The experiment proves that the control theory of the six-wheel legged chassis wheel-leg hydraulic cylinder can effectively improve the stability of the chassis,

and the smooth steering of the chassis could be achieved.

4) In the following work, fuzzy PID control will be presented for the tipping condition of the six wheel-legged chassis, and the stability of the chassis simulated by fuzzy PID control on a 30° slope is compared with the stability under fuzzy control, furthermore, the effectiveness of fuzzy PID control will be verified through prototype tests.

Acknowledgements

This work was supported by Fundamental Research Funds for the Central Universities (Grant No.2015ZCQ-GX-01) and National Key Project(2016YFE0203400-04).

R E F E R E N C E S

[1] *Sh. Wang, L. Geng.* Development situation and countermeasures of agricultural mechanization in hilly and mountain areas[J]. Journal of Agricultural Engineering, 2016 ,5(6) : 1-4.

[2] *He Peng, W. Ma, E. Zhao, et al*. Design and physical model experiment of body leveling system for roller tractor in hilly and mountainous region[J]. Transactions of the Chinese Society of Agricultural Engineering(Transactions of the CSAE), 2018 , 34(14): 36 − 44.

[3] *X. Zhou, Ahong Lai, C. Zhou, et al*. Advances in ecological logging of mountain forest[J]. Journal of Forest and Environment,2015,35(2):185-192.

[4] *Yue Zhu，Jiangming Kan，Wenbin Li , et al*. A novel forestry chassis with an articulated body with 3 degrees of freedom and installed luffing wheel-legs[J]. Advanced in Mechanical Engineering,2018,10(1):1-10

[5] *Yue Zhu，Jiangming Kan，Wenbin Li , et al*. Strategies of traversing obstacles and the simulation for a forestry chassis[J]. International Journal of Advanced Robotic Syestem,2018,10(1):1-10

[6] *Q. Zhu, C. Xiao, H. Hu.* Multi-sensor based online attitude estimation and stability measurement of articulated heavy vehicles[J]. Sensor, 2018 13:18(1).

[7] *M. Ashfaq Ali, C. Kim, S. Kim, et al*. Lateral acceleration potential field function control for rollover safety of multi-wheel military vehicle with in-wheel-motors[J]. International Journal of Control, Automation and Systems, 2017 15(2):837-847.

[8] *Z. Yao, G. Wang, X. Li, et al*. Dynamic simulation for the rollover stability performances of articulated vehicles[J]. Journal of Automobile Engineering, 2014 228(7):771-783.

[9] *X. Li, G. Wang, Z. Yao, et al*. Research on lateral stability and rollover mechanism of articulated wheel loader[J]. Mathematical and Computer Modelling of Dynamical Systems, 2014, 20(3): 248-263.

[10] *X. Li, G. Wang, Z. Yao, et al*. Dynamic model and validation of an articulated steering wheel loader on slopes and over obstacles[J]. Vehicle System Dynamics, 2013, 51(9), 1305-1323.

[11] *Y. OuYang, L. Li, Tang, et al*. Design and Experimental Research on Crawler Chassis of Oil Tea Plantation Tending Machine[J]. Journal of Northwest forestry University, 2018,33(2) : 252-256.

[12] *H. Tian, Z. Fang, Y. Zhou, et al*. Analysis and Simulation for Wheel-legged Robot Tumble Stability[J]. Journal of System Simulation, 2009，(13)：4032-4037.

[13] *H. Tian, Z. Fang, Y. Zhou, et al*. Analysis and Control for Tumble Stability of Wheel-Legged Robots[J]. Robot, 2009, 31(02)：159-165.

[14] *Z. Wang, W. Ma, H. Li,* et al. Design and Analysis of Hydraulic Leveling System in Hillside Tractor Body[J]. Hydraulics Pneumatics & Seals, 2017(1 0)：76－80.

[15] *S. Cao, L. Wang, T. Liu, et al*. Determination of the Main Parameters of Vehicle-servo Mobile Tree-measuring Scanner Mounts and Vehicle[J]. Journal of Northwest forestry University, 2017,32（6）：178-183.

[16] *D. Han, Yu Cao, S. Tong,* et al. Tong S Research on the motion deviation of the active gait chassis cross the obstacle used in the forestry based on differential kinematics[J]. Journal of Forest and Environment, 2019,39(5):554-560.

[17] *Z. Sun, J. Liu, C., et al*. Stability analysis and gait planning for luffing wheel-legged robot during intelligent obstacle-surmounting process[J]. Transactions of the Chinese Society of Agricultural Engineering (Transactions of the CSAE),2015, 31(16): 1－7.

[18] *Jun Li.* Kinematics Analysis on Stanford Arm Based on Screw Theory[J]. Journal of Tianjin University of Science & Technology, 2010,25（4）：73-75.

[19] *Z. Li, Z. Sun, J. Liu, J. Kan, C. Yu.* Stability analysis and control for a wheel-legged robot[J]. International Standard Serial Number, 2018, 80(2):15-26.

[20] *D. Zhu, Y. Fang.* Displacement Analysis and Synthesis of Parallel Manipulator via Screw Theory[J]. Robot, 2005，27(6)：539–544.

[21] *Lei Zhang, L. Zhou.* Steady Posture Adjustment of Hexapod Bionic Robot[J]. Mechanical Science and Technology for Aerospace Engineering, 2019,38（5）：670-676.

[22] *D. Zhao, D. Wang, Y. Cheng, et al*. Stability Analysis of Static Secondary Tilting of Articulated Steering Tractor[J]. Journal of Agricultural Machinery, 1994,25（01）：21-26.

[23] *T. Cai, M. Dong, S. Cui, ,et al*. Stability Evaluation of Loaders Based on Stability Degree[J]. Coal Mine Machinery, 2012,33（09）：78-80.

[24] *Yue Zhu, J. Kan.* The design of forestry chassis whit articulated body of three degrees of freedom and analysis of its obstacle surpassing ability[J]. Journal of Beijing Forestry University, 2016, 38(5)：126-132.

[25] *S. Chen.* Discussion on the Relationship between Hilly Lands Slope and Forestry Policy Implement[J]. East China Forest Management, 2009,23（01）：17-18.

[26] *Fen Chen, et al*. Terrain Analysis Based on GIS in Fujian Province[J]. Journal of East China Institute of Technology, 2009,32（02）：186-187.